

# Preparation of cationic polyacrylamide microsphere emulsion and its performance for permeability reduction

Guo Aijun<sup>1</sup>, Geng Yiran<sup>1</sup>, Zhao Lili<sup>1</sup>, Li Jun<sup>2</sup>, Liu Dong<sup>1</sup> and Li Peng<sup>1\*</sup>

<sup>1</sup> State Key Laboratory of Heavy Oil Processing and College of Chemical Engineering, China University of Petroleum (East China), Qingdao, Shandong 266580, China

<sup>2</sup> Technical Department of Ethylene Complex, Petrochina Dushanzi Petrochemical Company, Karamayi, Xinjiang 833600, China

© China University of Petroleum (Beijing) and Springer-Verlag Berlin Heidelberg 2014

**Abstract:** In this paper, cationic polyacrylamide microspheres (CPAM) were synthesized using acrylamide (AM) and methacryloyloxyethyl trimethyl ammonium chloride (TMAEMC) as monomers, ammonium sulfate as dispersant, poly(acryloyloxyethyl trimethyl ammonium chloride) (PAETAC) as dispersion stabilizer, and ammonium persulfate as initiator. The synthetic method was dispersion polymerization. The effects of monomer ratio (AM/TMAEMC), dispersant concentration, and dispersion stabilizer dosage on dispersion polymerization were systematically studied to determine the optimal preparation conditions. The structure and viscosity of the synthesized polymer were characterized by FTIR and capillary viscometry, respectively, and the particle sizes and distribution of the polymer microspheres were characterized by microscopy and dynamic light scattering, respectively. Finally, flow tests were conducted to measure the permeability reduction performance of the microspheres at various concentrations in sand packs with different permeability. Results show that CPAM emulsion of a solids content of 1wt% has excellent performance in low-to-medium permeability formations (< 1,000 mD), and the efficiency may reach above 90%.

**Key words:** Dispersion polymerization, cationic polyacrylamide microspheres, profile modification, permeability reduction

## 1 Introduction

During a secondary or enhanced oil recovery process, a substantial amount of oil may be bypassed by the injected fluid due to reservoir heterogeneity and the water cut of the produced fluids may be very high (Yu et al, 2011; Xiao and Wang, 2003; Fletcher et al, 1992; Liu et al, 2006). In order to enhance oil recovery, the widely used method is injecting water cutoff materials to control formation permeability and then to divert the follow-up injected fluid into the unswept zones, without damaging oil productivity (Hou et al, 2011; Lu et al, 2012; Shi et al, 2010; 2012; Dong et al, 2010). So it is necessary to synthesize a new water cutoff material to reduce water cut of produced fluids and improve oil-producing efficiency in formations (Fielding et al, 1994; Ning et al, 2007; Lin et al, 2008; 2009; Lu et al, 2010; Feng et al, 2010; Wang and Li, 2011; Qiao et al, 2012).

Polymer microspheres are newly developed water cutoff material. After hydration, swollen polymer microspheres

progressively adsorb and deposit in pore throats to closure fluid channels in the formations. There are many advantages for such permeability control treatment: the dispersed polymer microsphere emulsion has relatively low viscosity; formation water produced in oilfields may be used to prepare the polymer microsphere emulsion; and the most important is that the microspheres may be injected into formations continuously (Lei et al, 2011; Lin et al, 2003; 2011a; 2011b). However, most polymer microspheres are nonionic, showing weak interaction with clay. In order to enhance the interaction between polymer microspheres with clay, this investigation tries to incorporate cationic monomer into polymers.

Water dispersion polymerization is also a newly developed process for synthesizing polymer microspheres. This technology is simple in operation, and water is used, instead of organic solvent, to dissipate heat during reaction; hence, secondary pollution and environmental impact can be reduced. Therefore, research into water dispersion methods has important theoretical and practical values (Cho et al, 2002; Grazon et al, 2011; Semsarilar et al, 2012; Wang et al, 2011a; 2011b; 2011c; Liu et al, 2011; 2012; Ondaral et al,

\*Corresponding author. email: Lip@upc.edu.cn

Received February 13, 2014

2010; Song et al, 2003; Wu et al, 2008).

## 2 Experimental

### 2.1 Experimental materials

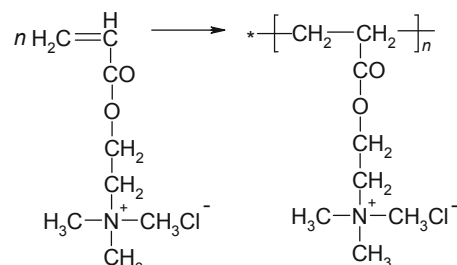
Acrylamide (AM, 99.0%), ammonium sulfate (AS, 99.0%), ammonium persulfate (APS,  $\geq 98.0\%$ ), *N,N'*-methylene diacrylamide (MEDAM, 96.0%), and sodium bicarbonate (99.8%) used in experiments were all purchased from the China National Medicines Corporation Ltd.; methacryloyloxyethyl trimethyl ammonium chloride (TMAEMC, 75.0wt% in water) and acryloyloxyethyl trimethyl ammonium chloride (AETAC, 75.0wt% in water) were purchased from the Penglai Spark Chemical Co., Ltd. AM and TMAEMC were used as monomers, AS and sodium bicarbonate as dispersants, and MEDAM as a crosslinker.

### 2.2 Preparation of cationic polyacrylamide microspheres

#### 2.2.1 Synthesis of a cationic dispersion stabilizer, poly(acryloyloxyethyl trimethyl ammonium chloride) (PAETAC)

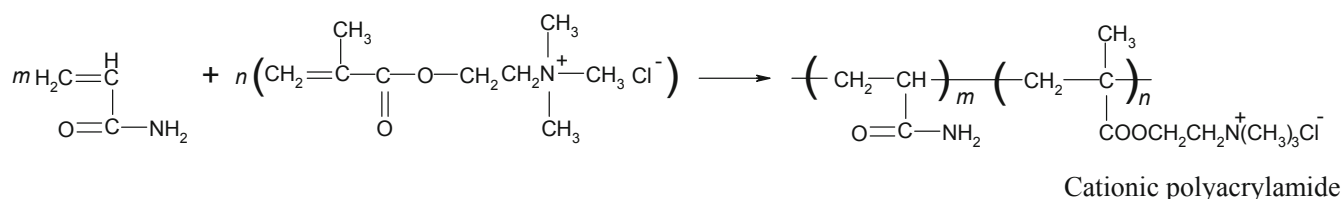
Two grams of AETAC was dissolved in 50 mL deionized water, which was then added to a three-necked flask. Nitrogen was kept flowing through the flask for 45 min and then the bath temperature was increased to 60 °C. APS, as an initiator, was added to the flask so that the reaction took place at this temperature for 1-2 h under stirring. Afterwards the reaction temperature was further increased to 75 °C and the reaction time was extended for about 3 h at this temperature. Nitrogen

was kept flowing during the whole synthesis process, and the final product, poly(acryloyloxyethyl trimethyl ammonium chloride) (PAETAC), was a viscous, brown liquid. The reaction equation of the cationic stabilizer is described as follows:



#### 2.2.2 Synthesis of cationic polyacrylamide microspheres (CPAM)

Monomers of AM and TMAEMC were weighed and put into a three-necked flask. Then ammonium sulfate, sodium bicarbonate, synthesized PAETAC solution, and deionized water were added and nitrogen was kept flowing for 20 min. After the temperature was increased to 50 °C, APS was added dropwise. When the reaction was over, the reaction mixture was cooled to room temperature for discharging. The crude product was a white emulsion with good fluidity and stability. Acetone was added to the crude product slowly, and the CPAM precipitated at the bottom gradually. After filtration, the CPAM was dissolved in deionized water again, and then precipitated by acetone; this process was repeated three times. At last, the CPAM was dried in an oven at 50 °C for 24 h. The main reaction is described as follows.



### 2.3 IR characterization

The copolymer after purification was dried to constant weight and pressed with KBr to disc form, and then a Fourier transform infrared spectrometer (NEXUS, Nicolet Co., USA) was used to characterize the cationic acrylamide polymer structure.

### 2.4 Determination of viscosity of the copolymer

The apparent viscosity of the crude product was determined with a NDJ-1 rotary viscometer. The dried CPAM was dissolved in deionized water to prepare a CPAM emulsion with a solids content of 1% (w/v, 0.01g/mL), and the viscosity of this emulsion is the intrinsic viscosity of cationic polyacrylamide.

### 2.5 Morphology of CPAM before and after hydrolysis

The purified CPAM was dissolved in deionized water

to obtain a dispersion system with a solids content of 1%, and NaOH solution was used to adjust the pH to 9. Then the sample was hydrated for 24 h at 65 °C. The morphology of CPAM in water before and after hydrolysis was observed with an inverted fluorescence microscope (XP-221, Jiangnan Yongxin Co.).

### 2.6 Particle size of CPAM

CPAM dispersions before and after hydrolysis were prepared as above, and 1 mL dispersions were put in a dynamic light scattering analyzer which was pre-heated for 30 min, and the microsphere sizes of CPAM in water were measured.

### 2.7 Performance of CPAM emulsion for permeability reduction

The porous media used was compacted packs of quartz sand (100-200 mesh). The sand packs were 52 cm long and 2.6

cm in diameter.

CPAM emulsions were prepared by dissolving CPAM in deionized water, and the salinity of the emulsions was adjusted with NaCl, KCl, MgCl<sub>2</sub>, and CaCl<sub>2</sub>.

The performance of CPAM emulsion for permeability reduction was investigated with the equipment shown schematically in Fig. 1 and the experimental procedures are described as follows:

1) The sand pack was dried, evacuated and saturated with water at a rate of 1 mL/min in order to determine its pore volume (PV), porosity and permeability. During water injection the pressure was recorded every 2 min.

2) 0.3 PV CPAM emulsion was injected into the sand pack at a rate of 1 mL/min and the pressure was monitored.

3) The sand pack was taken out of the core holder and placed in a 65 °C oven.

4) After 24 h, the sand pack was removed from the oven and cooled to room temperature.

5) The sand pack was installed at the core holder and then water was injected at a rate of 1 mL/min until the injection pressure was stabilized. During water injection the temperature and pressure were recorded every 2 min. Finally the permeability and permeability reduction of the sand pack after treatment were calculated.

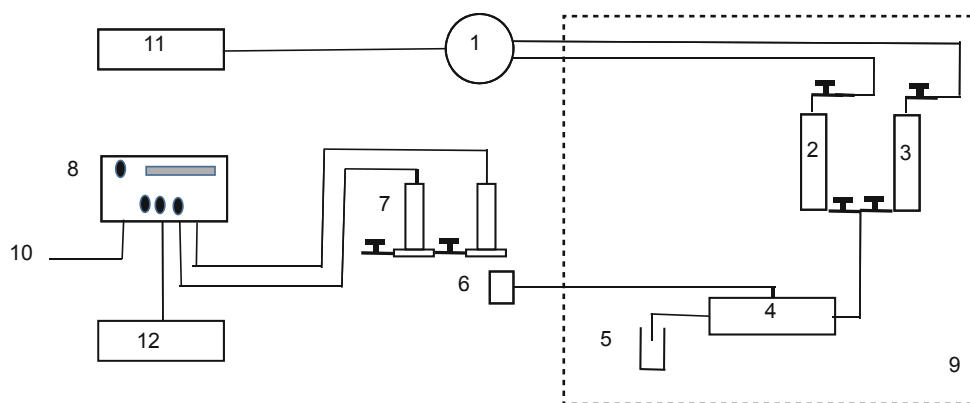


**Fig. 1** Experimental apparatus for flow experiments

1-6-way valve; 2-CPAM emulsion tank; 3-water tank; 4-core holder; 5-beaker; 6-ring pump; 7-pressure sensor; 8-digital pressure instrument; 9-constant temperature bath; 10-power; 11-micro-pump; 12-computer

## 3 Results and discussion

### 3.1 Dispersion polymerization of CPAM

CPAM was synthesized in laboratory and the effects of monomer molar ratio, stabilizer concentration, and APS concentration on polymerization reaction were investigated.

#### 3.1.1 Dispersion stabilizer concentration

The effect of stabilizer (PAETAC) concentration on aqueous dispersion polymerization was investigated under the following reaction conditions: total monomer concentration (AM and TMAEMC), 15wt%; AM/TMAEMC molar ratio, 8:2; APS concentration, 1wt%; AS concentration, 30wt%; and reaction temperature, 50 °C.

Table 1 shows the effect of PAETAC concentrations.

With an increase in the PAETAC concentration, the intrinsic viscosity of the cationic polyacrylamide emulsion decreased, while the apparent viscosity of the crude product increased when the PAETAC concentration was 0.5-0.6 g/g-monomer; when the PAETAC concentration was lower than 0.4 g/g-monomer, the crude product was uneven and unstable; when the PAETAC concentration was more than 0.5 g/g-monomer, the obtained CPAM were substantially spherical, and most of these particles were within the range of tens of nanometers, with an even distribution. If the PAETAC concentration continued to increase, the particle sizes of the obtained CPAM were reduced accordingly, therefore, the optimal PAETAC concentration adopted in the experiment was 0.5 g/g-monomer.

**Table 1** The effect of PAETAC concentration on CPAM dispersion polymerization

No.	PAETAC concentration g/g-monomer	Intrinsic viscosity of CPAM emulsion, dL/g	Viscosity of CPAM crude product, mPa·s	Morphology and stability of the crude product
1	0.3	—	—	Gel appeared in the early stage of polymerization
2	0.4	3.27	800	White-pink emulsion with good fluidity, a layer of CPAM was separated after standing
3	0.5	3.02	3150	White-pink emulsion with fluidity, no separation
4	0.6	2.88	3200	White-pink emulsion with fluidity, no separation

### 3.1.2 AM/TMAEMC molar ratio

The effect of the AM to TMAEMC molar ratio was investigated under the following conditions: total monomer

concentration of 15wt%, APS concentration, 1wt%; AS concentration, 30wt%; reaction temperature, 50 °C. The experimental results are listed in Table 2.

**Table 2** Effect of AM/TMAEMC molar ratio on CPAM dispersion polymerization

No.	AM/TMAEMC molar ratio	Intrinsic viscosity of CPAM, dL/g	Viscosity of CPAM crude product, mPa·s	Morphology and stability of the crude product
5	9:1	3.54	Very viscous	White jelly
6	8:2	3.02	3150	White-pink emulsion with fluidity, no separation
7	7:3	2.74	850	Dark pink emulsion with fluidity, no separation
8	6:4	2.61	350	Brown-pink emulsion with good fluidity, a layer of CPAM was separated after standing, unstable

Table 2 indicates that when the AM/TMAEMC molar ratio was in a range from 9:1 to 6:4, the intrinsic viscosity of CPAM emulsion decreased with a decrease in the AM/TMAEMC molar ratio. With a high concentration of TMAEMC, collisions among monomers decreased due to electrostatic repulsion, so the growth of molecular chains was restricted, and thus the intrinsic viscosity of the CPAM emulsion reduced as well as the apparent viscosity. Therefore,

an AM/TMAEMC molar ratio of 8:2 was selected to synthesize cationic polyacrylamide.

### 3.1.3 AS concentration

At a total concentration of monomers of 15wt%, APS concentration of 1wt%, AM/TMAEMC molar ratio of 8:2, and reaction temperature of 50 °C, the effect of the AS concentration during polymerization reaction was investigated, and the results are shown in Table 3.

**Table 3** Effect of AS concentration on CPAM dispersion polymerization

No.	AS concentration wt%	Intrinsic viscosity of CPAM emulsion, dL/g	Viscosity of CPAM crude product, Pa·s	Morphology and stability of the crude product
9	25	2.58	Poor fluidity	Gelatinous
10	27	2.92	13000	White-pink emulsion with fluidity
11	30	3.04	12500	White-pink emulsion with fluidity
12	33	2.79	4400	White-pink emulsion with fluidity, no separation

Table 3 indicates that the AS concentration had a significant effect on the intrinsic viscosity of the CPAM emulsion. As the AS concentration increased, the intrinsic viscosity first increased and then decreased. The reason is as follows: When the AS concentration is relatively low, the salting-out effect is weak and the reaction mainly takes place in the continuous phase. Therefore, the relative molecular weight of the copolymer is low. With an increase in the AS concentration, the polymerization may occur in the polymer phase, gradually transferred from the continuous water phase, in which the gel effect may exist during the transformation. Therefore, the growth time of free radicals in the polymer phase may be long, so the molecular weight of the copolymer increases as well. However, if the AS concentration is higher than 30%, the reaction may take place in the water phase again, but not the polymer phase, which results in a reduction of the molecular weight of cationic polyacrylamide. The above analysis indicates that 27wt%-30wt% sulfate nitrate solution will help to obtain polymer products with uniform particle size and good stability.

Therefore, the optimal synthesis conditions are as follows: the total concentration of monomers of 15wt%; AM to TMAEMC molar ratio of 8:2; APS concentration of 1wt%;

reaction temperature of 50 °C, and an AS concentration of 30wt%.

## 3.2 Characterization of CPAM

### 3.2.1 Infrared spectrum analysis

It can be seen from the IR spectrum of CPAM (Fig. 2) that the absorption peak at 3,476 cm<sup>-1</sup> and 3,180 cm<sup>-1</sup> are peaks of symmetric and asymmetric stretching vibrations of N—H bonds of amide, respectively. The absorption at 1,680 cm<sup>-1</sup> is the symmetric stretching vibration of C=O in amide, and absorption peak at 1,740 cm<sup>-1</sup> is due to the C=O stretching vibration for acyloxy. The absorption peak at 1,402 cm<sup>-1</sup> is attributed to bending vibration of methylene in a cationic monomer —CH<sub>2</sub>—N<sup>+</sup>(CH<sub>3</sub>)<sub>3</sub>, and the sharp absorption peak at 1,109 cm<sup>-1</sup> is characteristic of the C—O vibration in ester groups.

### 3.2.2 Inverted fluorescence microscope observation

The CPAM were hydrolyzed at 65 °C and alkaline conditions (pH=9), and an inverted fluorescence microscope was used to observe the changes of CPAM in water before and after hydrolysis, as shown in Fig. 3.

Fig. 3(a) shows the morphology of the CPAM just dissolved in water observed with the inverted fluorescence

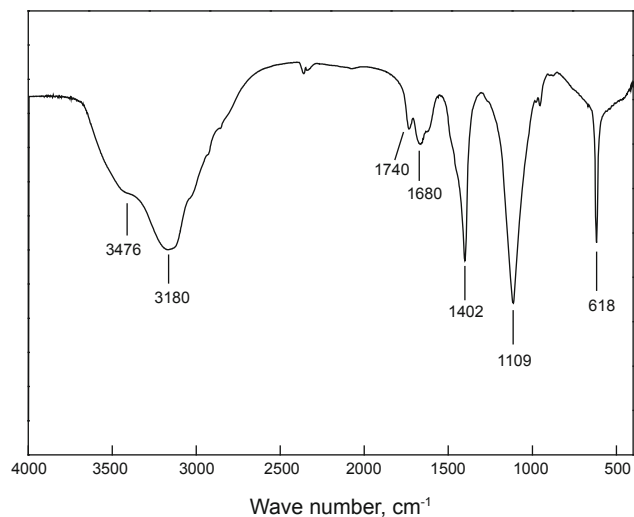
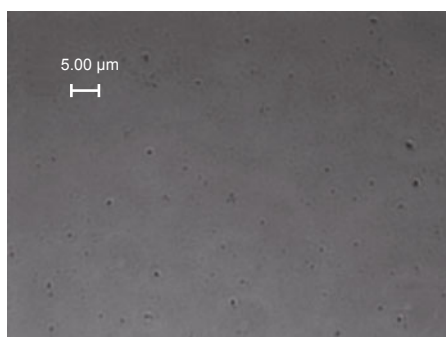
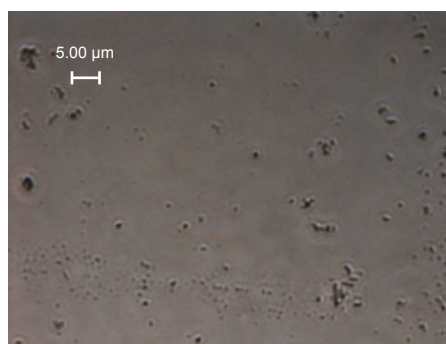


**Fig. 2** Infrared spectrum of CPAM



(a) Prior to hydrolysis



(b) After hydrolysis

**Fig. 3** Inverted fluorescence microscopy images of CPAM before and after hydrolysis

microscope, where the polymer particles are very small and barely visible in this figure.

Fig. 3(b) shows the morphology of CPAM after swelling in water at pH=9 for 24 h. Many micrometer-sized spherical particles were observed. Therefore, the synthetic polymer microspheres exhibit significant swelling behavior caused by hydrolysis under alkaline conditions and the particle size may swell from nanometers to microns which meets the requirements for reducing the reservoir permeability.

### 3.2.3 Dynamic light scattering analysis

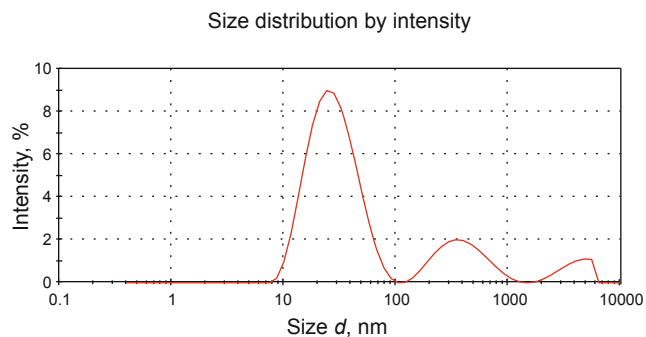
Fig. 4 shows the particle size distribution of CPAM synthesized under the optimal conditions. As can be seen from the figure, the particle sizes were mainly distributed from 7 nm to 100 nm, with an average diameter of 31 nm.

Fig. 5 (a) shows the particle diameter distribution by intensity of CPAM synthesized under the optimum conditions, dissolved, dispersed and swollen in water at pH=9. As can be seen from the figure, the particles were mainly distributed in the range of 160-1,020 nm, with an average particle size of 348 nm. Fig. 5(b) is the corresponding particle distribution by number, where the proportion of particle numbers reached 100% in 140-1,000 nm, without other peaks. This shows that the CPAM hydrolysis and swelling did occur at pH=9, leading to a tenfold increase in diameter. The observed results agree with the theoretical analysis.

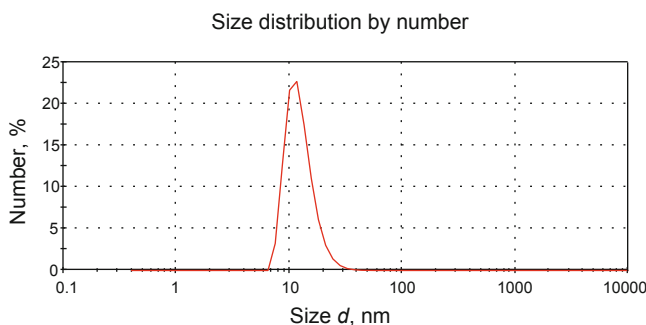
Fig. 6(a) shows the particle diameter distribution by intensity of CPAM swollen in water at pH=11. The CPAM used were synthesized under optimal conditions. It can be seen from the figure that the particles were mainly distributed in 150-1,200 nm, with an average particle size of 346 nm. Fig. 6(b) is the corresponding particle distribution by number. Within the range of 130 to 1,000 nm, the number of CPAM reached 100% without other peaks.

It can be calculated from Figs. 5 and 6 that CPAM expanded 11.3 and 11.2 times of the initial size at pH=9 and pH=11 conditions, respectively.

To sum up, the CPAM synthesized under optimized conditions were found to be ten nanometers to several tens of nanometers in diameter before hydrolysis; when they



(a) Particle size distribution by intensity



(b) Particle size distribution by number

**Fig. 4** Particle size distribution of CPAM in water (pH=7) prior to hydrolysis

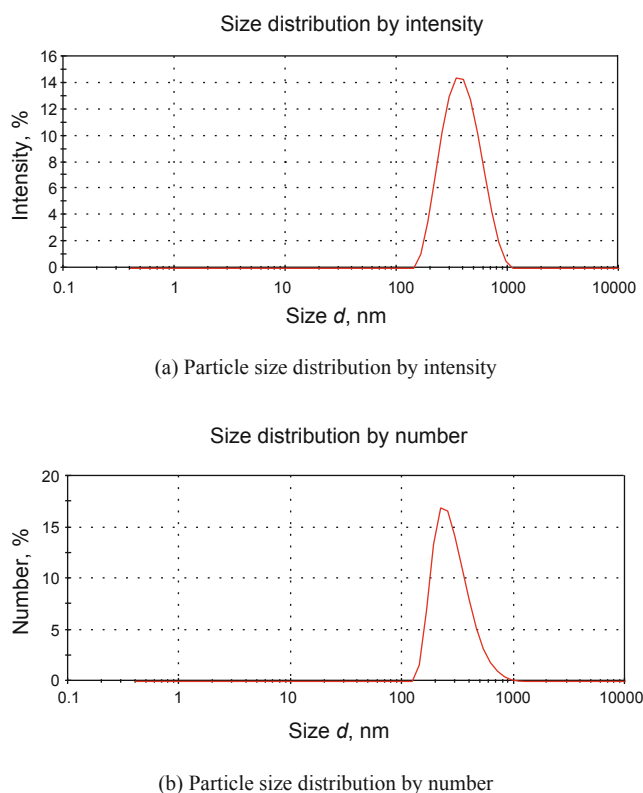


**Fig. 5** Particle size distribution of CPAM after hydrolysis in water at pH=9

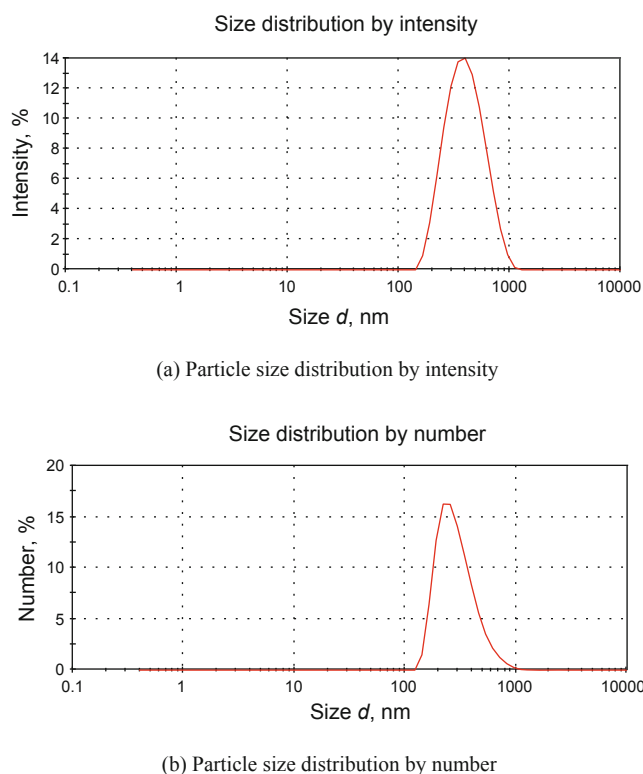


**Fig. 6** Particle size distribution of CPAM after hydrolysis in water at pH=11

hydrolyzed and swollen in water for 24 h under alkaline conditions, their particles were of 300-400 nm, and there is no significant difference between diameters of the hydrolyzed

CPAM swelling in pH=9 and pH=11 solutions.

### 3.3 Permeability reduction performance of CPAM

#### 3.3.1 Effect of CPAM concentration

CPAM synthesized under optimum conditions were selected to formulate emulsions with a solid content of 0.3wt%, 0.5wt%, 1wt%, and 2wt%. The sand packs used had an average porosity of 26.9% and permeability of 339-504 mD.

Fig. 7 shows curves of injection pressure versus with time (injected volume) before and after CPAM injection. Fig. 7(a) shows that after 0.3 PV CPAM emulsion of 0.3wt% solids content was injected into the sand pack, the injection pressure gradually increased to a peak value of 2.0 MPa and then decreased to a plateau level of 1.8 MPa when water was continuously injected. This means that after water breakthrough, which occurred at 170 min, some polyacrylamide microspheres were forced to move forward with water, and deposited and plugged other pores and pore throats in the sand pack. In the end, the injection pressure stabilized at about 1.8 MPa. Fig. 7(b) shows that for the sand pack treated with 0.5wt% CPAM emulsion the injection pressure gradually increased to a peak value of 8.0 MPa and then decreased to a plateau level of 5.0 MPa when water was continuously injected. Fig. 7(c) and Fig. 7(d) indicate that when the solids contents in the emulsions were respectively 1.0wt% and 2.0wt%, the variations of injection pressure with time were similar in the follow-up flow tests. At the beginning, the injection pressure increased slowly, but after 1 PV water was injected, the injection pressure increased sharply. After injecting about 2 PV water, the injection pressure gradually stabilized at about 12 MPa.

This is because the polyacrylamide microspheres continued to swell due to hydrolysis, and the swollen microspheres may adsorb and deposit in the pores and pore throats so as to block the flow channels well. Moreover, the swollen polyacrylamide microspheres had a certain ability to block the flow channels for a long time without being displaced by flooding fluids. Injection of CPAM emulsion of higher solids content into the sand pack means that more polyacrylamide microspheres absorbed and deposit in the pores and pore throats. For formations with similar permeability, more microspheres lead to higher injection pressure.

Table 4 lists the permeability reduction performance of CPAM emulsions with different solids contents. As can be seen from the table, when the solids contents were 0.5wt%, 1.0wt% and 2.0wt%, respectively, the rate of permeability reduction of all the sand packs were more than 99%. Therefore, from the economic perspective, the CPAM emulsion of solids content of 0.5wt% or 1wt% was recommended.

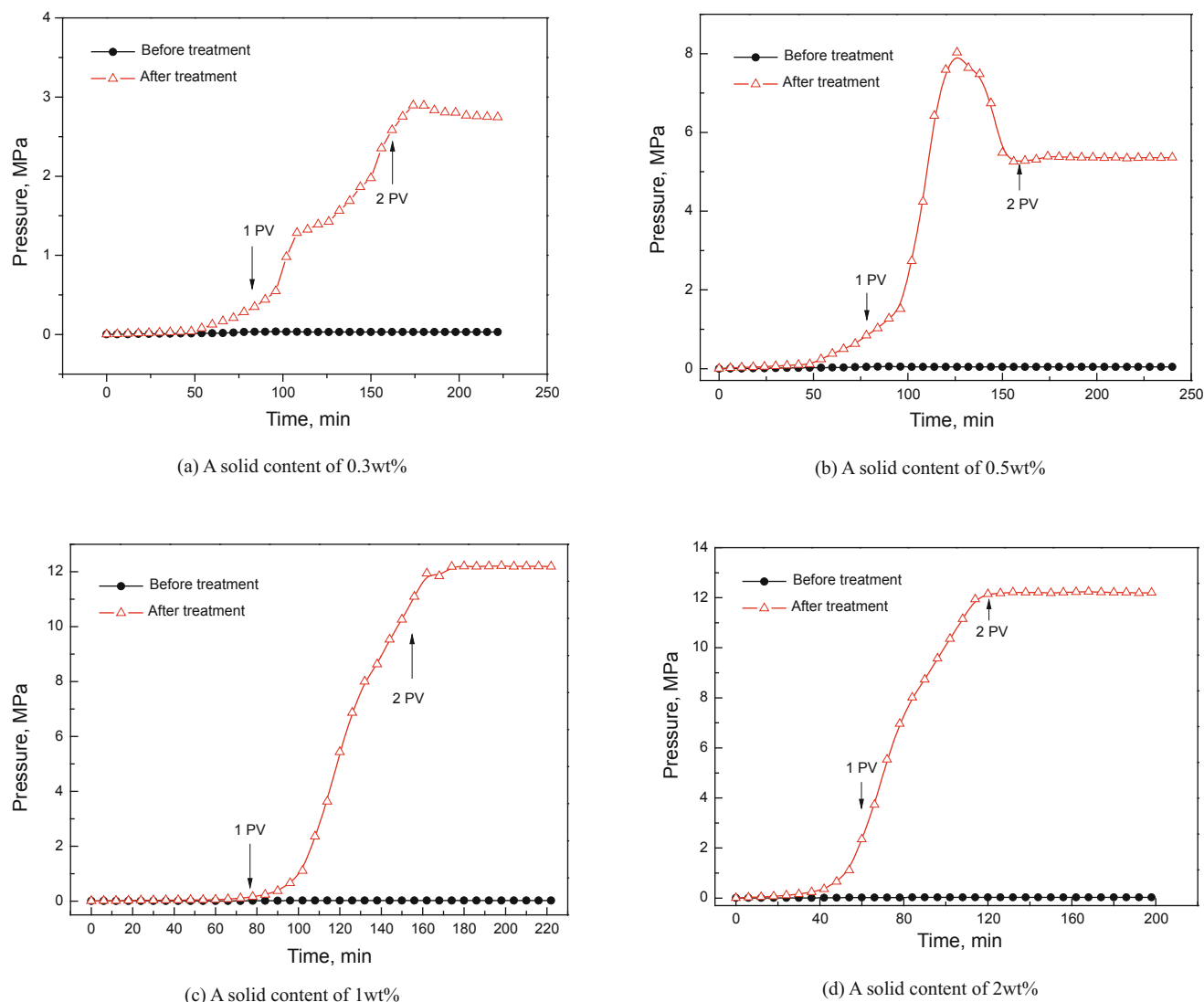


**Fig. 7** Curves of injection pressure with time before and after treatment with CPAM emulsions of different solids contents

**Table 4** Permeability reduction performance of CPAM emulsion

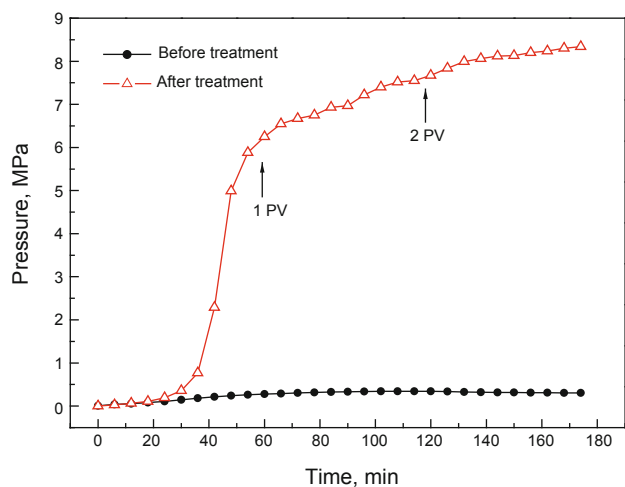
No.	Solids content in CPAM emulsion, wt%	Pore volume L	Initial porosity %	Initial permeability to water $K_{0s}$ , mD	Post-treatment permeability to water $K_s$ , mD	Rate of permeability reduction, %
1	0.3	0.30	27.1	483	40.8	91.6
2	0.5	0.29	26.5	339	2.78	99.2
3	1.0	0.30	27.2	702	1.28	99.8
4	2.0	0.30	26.9	504	1.20	99.8

### 3.3.2 Effect of formation permeability

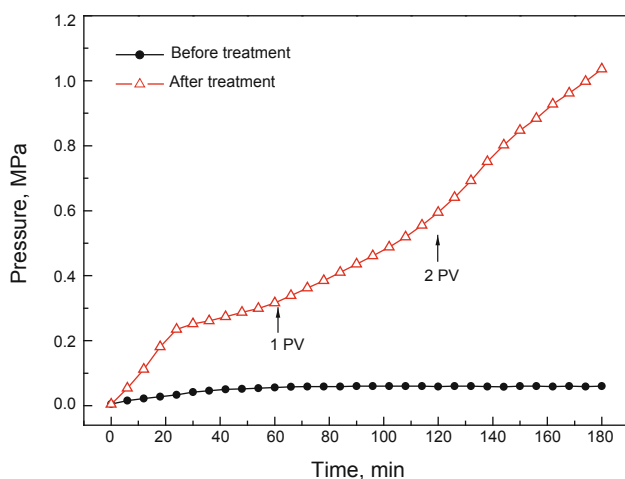
After hydrolysis at 65 °C for 24 h, 0.3 PV CPAM emulsion with a solids content of 1wt% was injected into the sand packs with different permeability. Before and after CPAM emulsion injection, flow tests were conducted and the curves of injection pressure with time are shown in Fig. 7.

Fig. 7(a) shows that for low permeability formations treated with 0.3 PV CPAM emulsion, the injection pressure increased sharply before 62 min (1 PV water), and then slowed down. After 140 min, the pressure stabilized.

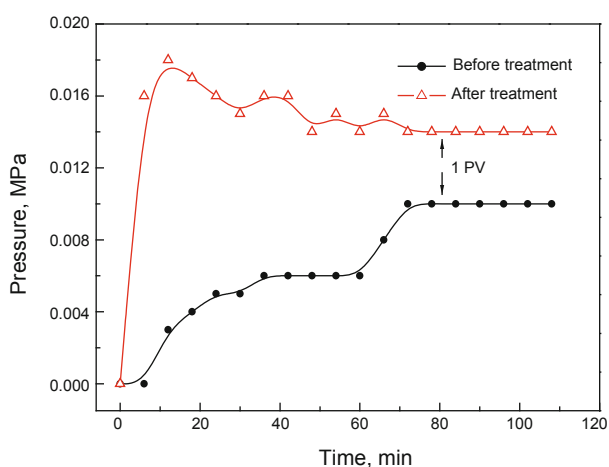
The CPAM may effectively reduce the permeability of low permeability formations. For medium permeability formations, the injection pressure increased slowly at the beginning, while grew fast after 2 PV water injection, and still presented a growing trend after 3 PV water was injected. Moreover, the injection pressure of entire process was not very high, less than 1.0 MPa. For high permeability formations, the maximum injection pressure was only 0.017 MPa, which was a little higher than the injection pressure of the sand pack before being treated with CPAM emulsion.



(a) Sand pack with low permeability of 53 mD



(b) Sand pack with medium permeability of 237 mD



(c) Sand pack with high permeability of 1427 mD

**Fig.8** Injection pressure of CPAM emulsion versus injection time in different permeability sand packs

Therefore, the CPAM emulsion could not effectively reduce the permeability of high permeability formations. Table 5 lists the permeability of sand packs before and after injection of CPAM emulsion. Table 5 shows that the CPAM emulsion

of a solids content of 1wt% may reduce the permeability of low-to-medium permeability formations by more than 90%; while for high permeability sand packs of over 1,000 mD, the CPAM emulsion performed poorly, reducing the sand pack permeability by less than 30%. Hence, the CPAM can be used in profile modification of low-to-medium permeability formations, but not in high permeability formations.

**Table 5** Performance of CPAM for permeability reduction of different permeability sand packs

No.	Pore volume, L	Initial permeability to water $K_{0}$ , mD	Porosity %	Post-treatment permeability to water $K$ , mD	Rate of permeability reduction %
7	0.22	53	19.9	2.07	96.1
8	0.30	237	27.3	14.4	93.9
9	0.33	1426	29.7	1030	27.8

### 4 Conclusions

Cationic polyacrylamide microspheres (CPAM) were synthesized using the dispersion polymerization method and were systematically characterized. Flow tests were conducted on sand packs before and after treatment with CPAM emulsions to investigate the performance of CPAM to control formation permeability. The following conclusions are drawn.

1) The optimized conditions for CPAM polymerization are as follows: the dosage of stabilizer (PAETAC) at about 0.5 g/g-monomer, AM to DMC molar ratio at 8:2, ammonium sulfate concentration at 27wt%-30wt%, APS (initiator) concentration at 1wt%, and reaction temperature at 50-55 °C. Under these conditions, a uniform polymer emulsion with higher viscosity and good stability was obtained.

2) Cationic polyacrylamide can be hydrolyzed under basic conditions of pH=9, and its particle sizes increase by more than ten times during hydrolysis. The swollen polyacrylamide microspheres are neat and regular.

3) The CPAM emulsion of a solids content of 0.5%-2.0% may effectively reduce the permeability of low-to-medium permeability formations, and 99% permeability reduction was achieved. While for high permeability formations exceeding 1,000 mD, only 28% permeability reduction was achieved.

### Acknowledgements

The authors are grateful for financial support from the National Natural Science Foundation of China (Grants Nos. 51203186, U1362101 and 51173203), the Converging Research Center Program funded by Korean Ministry of Education (2013K000415), and the Project of Science and Technology Program for Basic Research of Qingdao (No. 12-1-4-7-(6)-jch).

### References

Cho M S, Yoon K G and Song B K. Dispersion polymerization of acrylamide in aqueous solution of ammonium sulfate: synthesis and characterization. *Journal of Applied Polymer Science*. 2002. 83(7): 1397-1405  
 Dong Z X, Lin M Q, Wang H, et al. Influence of surfactants used in



- surfactant-polymer flooding on the stability of Gudong crude oil emulsion. *Petroleum Science*. 2010. 7(2): 263-267
- Feng Q H, Shi S B, Wang S, et al. Numerical simulation of profile control by clay particles after polymer flooding. *Petroleum Science*. 2010. 7(4): 509-514
- Fielding R C, Gibbons D H and Legrand F P. In-depth drive fluid diversion using an evolution of colloidal dispersion gels and new bulk gels: an operational case history of the North Rainbow Ranch unit. SPE/DOE Improved Oil Recovery Symposium, 17-20 April, 1994, Tulsa, Oklahoma (SPE/DOE 27773)
- Fletcher A J P, Flew S, Forsdyke I N, et al. Deep diverting gels for very cost-effective waterflood control. *Journal of Petroleum Science and Engineering*. 1992. 7(1-2): 33-43
- Grazon C, Rieger J, Sanson N, et al. Study of poly(*N,N*-diethylacrylamide) nanogel formation by aqueous dispersion polymerization of *N,N*-diethylacrylamide in the presence of poly(ethylene oxide)-*b*-poly(*N,N*-dimethylacrylamide) amphiphilic macromolecular RAFT agents. *Soft Materials*. 2011. 7(7): 3482-3490
- Hou J, Du Q J, Lu T, et al. The effect of interbeds on distribution of incremental oil displaced by a polymer flood. *Petroleum Science*. 2011. 8(2): 200-206
- Lei G L, Li LL and Nasr-El-Din H A. New gel aggregates to improve sweep efficiency during water flooding. *SPE Reservoir Evaluation & Engineering*. 2011. 14(1): 120-128
- Lin M Q, Han F X, Li M Y, et al. Study of plugging performance of LPS with nucleopore film. *Membrane Science and Technology*. 2003. 23(2): 11-14 (in Chinese)
- Lin M Q, Zhang C L, Zong H, et al. Influence of polymers on the stability of Gudao crude oil emulsions. *Petroleum Science*. 2008. 5(2): 159-162
- Lin M Q, Zhao Z H, Li M Y, et al. The effect of surface wettability of porous media on the plugging properties of LPS. *Acta Petrolei Sinica (Petroleum Processing Section)*. 2009. 20(5): 48-52 (in Chinese)
- Lin M Q, Dong Z X, Peng B, et al. Shape, size and plugging properties of crosslinked polyacrylamide microspheres. *Acta Polymerica Sinica*. 2011a. (1): 48-54 (in Chinese)
- Lin M Q, Guo J R, Xu F Q, et al. Study of the matching between cross-linked polymer microspheres and nuclear-pore membranes. *Advanced Materials Research*. 2011b. 160-162: 1346-1353
- Liu H Q, Zhang H L and Wang S L. Research on mechanisms of steam breakthrough and profile control design for steam soaking well. *Petroleum Science*. 2006. 3(3): 51-55
- Liu J, Wang C X and Wu Y M. Aqueous dispersion polymerization of acrylamide in ammonium chloride solution with water-soluble chitosan as a stabilizer. *Iranian Polymer Journal*. 2011. 20(11): 887-896
- Liu J, Wang C X and Wu Y M. Dispersion polymerization of acrylamide with water-soluble chitosan as the stabilizer. *Journal of Applied Polymer Science*. 2012. 125(2): 518-525
- Lu J, Peng B, Li M Y, et al. Dispersion polymerization of anionic polyacrylamide in an aqueous salt medium. *Petroleum Science*. 2010. 7(3): 410-415
- Lu X G, Liu J X, Wang R J, et al. Study of action mechanisms and properties of Cr<sup>3+</sup> cross-linked polymer solution with high salinity. *Petroleum Science*. 2012. 9(1): 75-81
- Ning Z F, Liu H Q and Zhang H L. Steam flooding after steam soak in heavy oil reservoirs through extended-reach horizontal wells. *Petroleum Science*. 2007. 4(2): 71-74
- Ondaral S, Usta M, Gumusderelioglu M, et al. The synthesis of water soluble cationic microgels by dispersion polymerization: their performance in kaolin deposition onto fiber. *Journal of Applied Polymer Science*. 2010. 116(2): 1157-1164
- Qiao R, Zhang R, Zhu W Q, et al. Lab simulation of profile modification and enhanced oil recovery with a quaternary ammonium cationic polymer. *Journal of Industrial and Engineering Chemistry*. 2012. 18(1): 111-115
- Semsarilar M, Ladmiral V, Blanzas A, et al. Cationic polyelectrolyte-stabilized nanoparticles via raft aqueous dispersion polymerization. *Langmuir*. 2012. 29(24): 7416-7424
- Shi L T, Ye Zhong B, Zhang Z, et al. Necessity and feasibility of improving the residual resistance factor of polymer flooding in heavy oil reservoirs. *Petroleum Science*. 2010. 7(2): 251-256
- Shi L T, Chen L, Ye Z B, et al. Effect of polymer solution structure on displacement efficiency. *Petroleum Science*. 2012. 9(2): 230-235
- Song B K, Cho M S, Yoon K J, et al. Dispersion polymerization of acrylamide with quaternary ammonium cationic comonomer in aqueous solution. *Journal of Applied Polymer Science*. 2003. 87(7): 1101-1108
- Wang B and Li M Y. Plugging properties of novel profile control agent carboxymethyl starch. *Journal of Petrochemical Universities*. 2011. 24(1): 86-88 (in Chinese)
- Wang X N, Yue Q Y, Gao B Y, et al. Kinetics of dispersion polymerization of dimethyl diallyl ammonium chloride and acrylamide. *Journal of Polymer Research*. 2011a. 18(5): 1067-1072
- Wang C X, Wang X X, Miao C B, et al. Preparation and properties of amphoteric polyacrylamide by seeded dispersion polymerization in ammonium sulfate solution. *Polymer Engineering & Science*. 2011b. 51(9): 1742-1748
- Wang X N, Yue Q Y, Gao B Y, et al. Dispersion copolymerization of acrylamide and dimethyl diallyl ammonium chloride in ethanol-water solution. *Journal of Applied Polymer Science*. 2011c. 120(3): 1496-1502
- Wu Y M, Chen Q F, Xu J, et al. Aqueous dispersion polymerization of acrylamide with quaternary ammonium cationic comonomer. *Journal of Applied Polymer Science*. 2008. 108(1): 134-139
- Xiao C M and Wang Z L. Review of profile and water plugging in oilfields. *Advances in Fine Petrochemicals*. 2003. 4(3): 43-46 (in Chinese)
- Yu H, Wang Y, Ji W, et al. Study of a profile control agent applied in an offshore oilfield. *Petroleum Science and Technology*. 2011. 29(12): 1285-1297

(Edited by Sun Yanhua)